

NUCLEAR EXPERIMENTAL TECHNIQUE

A Drift Tracker of the SVD-2 Setup

S. G. Basiladze^a, M. A. Baturitskii^b, G. A. Bogdanova^a, V. N. Bychkov^c, K. S. Viryasov^c,
V. Yu. Volkov^a, Ya. V. Grishkevich^a, P. F. Ermolov^a, E. G. Zverev^a, G. D. Kekelidze^c,
E. S. Kokoulina^c, A. V. Kubarovskii^a, A. K. Leflat^a, V. M. Lysan^c, V. V. Myalkovskii^c,
V. A. Nikitin^c, V. D. Peshekhonov^c, V. V. Popov^a, I. A. Rufanov^c, V. A. Sen'ko^d,
N. A. Shalanda^d, and A. Yu. Yukaev^d

^a Skobel'tsyn Institute of Nuclear Physics, Moscow State University, Vorob'evy gory 1, str. 2, Moscow, 119991 Russia

^b Research Center for Particle and High Energy Physics, Belarussian State University,
ul. M. Bogdanovicha 153, Minsk, 220040 Belarus

^c Joint Institute for Nuclear Research, ul. Joliot-Curie 6, Dubna, Moscow oblast, 141980 Russia

^d Institute for High Energy Physics, ul. Pobedy 1, Protvino, Moscow oblast, 142281 Russia

Received November 14, 2007

Abstract—The design and the characteristics of a drift tracker for the SVD-2 setup at the U-70 accelerator of the Institute for High Energy Physics (Protvino, Russia) are described. The drift tracker has been developed to improve the quality of track reconstruction in high-multiplicity events. It is composed of 2304 drift tubes with a diameter of 6 mm and a sensitive region 500–900 mm long. The distance between a track and the anode wire is determined from the drift time. The coordinate resolution and the detection efficiency of the tubes have been determined from the data of the accelerator run in 2006.

PACS numbers: 29.40.Cs, 29.85.+c

DOI: 10.1134/S0020441208030032

INTRODUCTION

A drift tracker has been developed for the spectrometer with a vertex detector (SVD-2) setup at the U-70 proton accelerator of the Institute for High Energy Physics (Protvino, Russia) [1]. The SVD-2 setup is used to study pp interactions at energies of 50–70 GeV in the “Thermalization” project [2]. This project is aimed at searching for and investigating high-multiplicity events in which effects of multiparticle quantum statistics manifest themselves. At an energy of 70 GeV, 20-ray events were observed in the MIRABEL hydrogen chamber. The kinematic limit of this reaction at this energy was 69 pions.

The SVD-2 setup was not initially intended for measuring high-multiplicity events. In the case in which tracks recorded by different subsystems are great in number, there are a variety of variants in which they can be matched. In the SVD-2, this leads to errors in determining the particle momenta. The use of the drift tracker, which measures tracks in the critical region between the vertex detector and the magnetic spectrometer, has made it possible to substantially reduce the probability of such errors.

EXPERIMENTAL SETUP

The head of the SVD-2 setup is shown in Fig. 1. The beam components of the trigger system were described in [3–5]. Scintillation counters C_1 and C_2 detect beam

particles, and a beam trigger is produced when a particle trajectory departs by <3 mm from the beam axis in the plane of counters C_3 and C_4 . The trajectory of beam particles is determined more precisely by microstrip detectors of beam station BS . The beam trigger activates the multiplicity analysis modules of trigger detector TD , which consists of 19 1.6-mm-thick conical scintillation counters located along a circle. The pulse heights from these counters are measured by fast two-bit analog-to-digital converters (ADCs) and are summed in a digital form. If the sum exceeds the preset threshold, a *High-multiplicity event* signal is produced.

The precision vertex detector (PVD) is composed of ten microstrip silicon detectors 300 μm thick located with a pitch of 50 μm . The four front planes comprise 640 32-mm-long strips, while the six back planes have 1024 51.2-mm-long strips. In the machine run of 2006, all the PVD planes were installed in pairs (Y, X), so that the strips of planes X and Y were located in horizontal and vertical planes, respectively. The other detectors of the SVD-2 setup have inclined planes labeled by indices U and V . They are turned around beam axis Z through angles of $+10.5^\circ$ and -10.5° with respect to the vertical position.

The charged particle momenta are measured by a wide-aperture magnetic spectrometer (WAMS). It contains an MC-7A electromagnet, which creates a homogeneous field of up to 1.18 T in a working volume of $3.0 \times 1.8 \times 1.3 \text{ m}^3$, and six triplets (UYV) of propor-

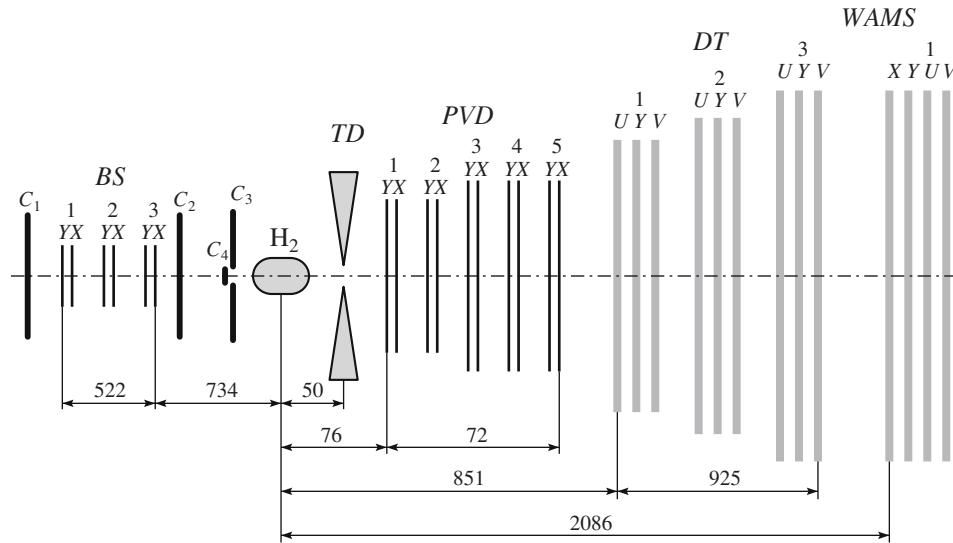


Fig. 1. Diagram of the SVD-2 setup head: (*BS*) beam station, (C_1 – C_4) beam counters, (H_2) liquid-hydrogen target, (*TD*) trigger detector, (*PVD*) precision vertex detector, (*DT*) drift tracker, and (*WAMS*) wide-aperture magnetic spectrometer.

tional chambers with a 2-mm pitch of anode wires (only the first triplet is shown in Fig. 1), which are housed in this volume. The sensitive area of the eight front-end chambers is 1 m^2 , while that of the other chambers is 1.5 m^2 . Without recourse to the PVD data, momenta from the ranges of 1–3, 3–8, and 8–13 GeV/ c can be measured with accuracies of 5.1, 2.3, and 1.4%, respectively.

As the multiplicity increases, the combinatorial background in matching the tracks measured by different detectors increases according to the quadratic law. The PVD and the WAMS are placed 2 m apart. Distortion of particle trajectories through multiple scattering on the base such as this leads to ambiguity in matching the track data when more than 12 tracks are recorded. To solve this problem, it was necessary that a detector with high detection efficiency, high coordinate resolution, and minimum distortions in particle trajectories be inserted between the PVD and the WAMS. A version of the detector design based on thin-walled drift tubes (i.e., straw tubes) has been selected. The development and commissioning of the drift tracker (DT) came to an end in 2006.

DESIGN OF THE DRIFT DETECTOR

The DT consists of three modules, each of which is a *UYV* triplet of double-layer straw chambers identical in size. The modules are placed one after the other with a spacing of 360 mm, and chambers in the modules are

separated by 100 mm. Number of tubes n and length l of their sensitive region in the chambers are as follows:

Module no.	n	l , mm
1	160	500
2	256	700
3	352	900

In the DT design, we used an assembly of planar straw chambers and a technology developed and employed in the COMPASS spectrometer [5, 6]. Tubes with an interior diameter of $6.02 (-0; +0.025)$ mm and $62\text{-}\mu\text{m}$ -thick walls are wrapped inside two kapton ribbons: an internal ribbon, XC160 kapton with a resistivity of $370 \Omega/\square$ and a thickness of $40 \mu\text{m}$, and an external ribbon, 100HN kapton with a thickness of $12.5 \mu\text{m}$ and an interior surface coated with an aluminum layer 500 \AA thick. Each chamber comprises two isolated planes of tubes glued to each other and separated by a kapton film ($300 \mu\text{m}$). The planes are shifted by the value of the radius and glued to the aluminum frame of the chamber. On the extension of the chamber, there are hermetically sealed gas collectors, inside which data readout cards are mounted on one side and anode voltage supply cards are placed on the other.

A gold-plated tungsten wire $30 \mu\text{m}$ thick is used as an anode. The wire is fixed in place inside the tube with the aid of end sleeves and metal–plastic terminal clamps. The limit of elasticity of the wire is 120 g. Measurements show that the tension of 95% of all the wires is in the range of 80–92 g.

To reduce the counting rate due to beam particles, insensitive zones have been created in the chambers. For this purpose, the middles of the six central wires of

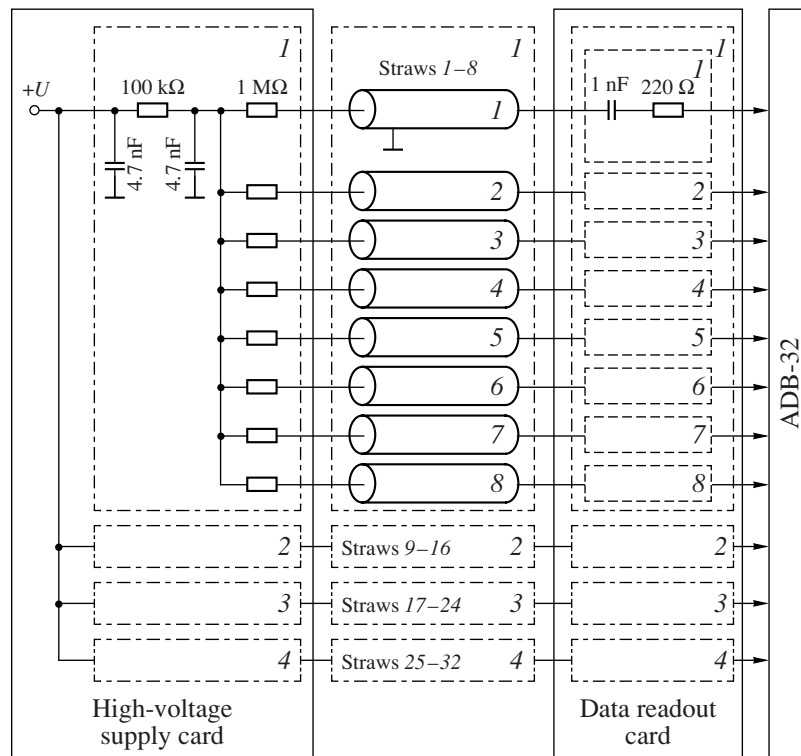


Fig. 2. Circuit diagram of the group of 32 chamber channels.

each chamber are sealed by melting into borosilicate glass capillaries [7] with a length of 12 mm, an outside diameter of 0.25 mm, and an inside diameter of 0.1 mm. Sealing is performed in two local zones of a capillary. The thickness of one layer of the chamber, averaged over the sensitive area, is 0.09% of radiation length X_0 ; in the zone of capillaries, it increases to 0.097% of X_0 .

The walls of the tubes are made of kapton, which is hygroscopic. To prevent the tubes from deforming as a result of possible increase in the air humidity, the chambers are covered on two sides by an aluminized Mylar film 20 μm thick. The protective volume produced thereby is continuously vented with dry carbon dioxide or nitrogen.

Additional positioning elements are installed in the chambers of the third module, which has the largest size. At a distance of 20 mm from the middle, the anode wires are supported by spacers. From the outside, the planes are wrapped by carbon ribbons glued to the tubes and the frames of the chambers.

CIRCUIT DIAGRAM OF THE CHAMBERS AND DIGITAL DATA ACQUISITION

To transmit the anode signals to the inputs of amplifiers, 32-channel data acquisition cards are mounted into one end of the chamber frames. High-voltage supply cards are fastened to the other end of the frames.

The circuit diagram of a group of 32 channels is shown in Fig. 2.

The high-voltage distribution circuit contains two-stage filters divided into groups with eight channels in each. These filters protect the inputs of the amplifiers from noise in the case of high-voltage discharges in the other channels of the detector.

The signals from the anode wires are transmitted through a 1-nF capacitor and a 220- Ω resistor to the connectors of ADB-32 amplifier-discriminator boards. The high value of the capacitors ensures a good uniformity of the channels. The 32-channel ADB-32 boards [8] are fixed on the ends of the chambers. They are based on AMPL-8.3 (a current amplifier) and DISC-8.3 (a level discriminator) chips and have the following parameters: input resistance, 50 Ω ; threshold of action, 1.2 μA ; low voltage differential signaling (LVDS) levels of the output potentials; and duration of the output pulse, 40 ns.

After being shaped, the pulses are transmitted over an 8-m-long ribbon multiconductor cable to the data acquisition equipment disposed in two MISS crates [9] at the control desk of the setup. The crates contain 64-channel time-to-digital converter (TDC) modules of the ПЭ-82 type, which measure the time interval from the pulse in the DT channel (the *Start* signal) to the *Common Stop* signal arriving from the trigger system. The range of measurements is 512 samples with a step of 2.2 ns. The module permits recording of as many as

five pulses in each channel. Data are read out into the computer via ПЭ-83 crate controllers over the Q bus.

EXPERIMENTAL CONDITIONS

A beam with a stretch of 1–2 s and an intensity of 10^6 s^{-1} was used in the experiment on the SVD-2 setup in the run of 2006. The beam width was $\sigma = 1.5 \text{ mm}$ in both directions. A total of 2×10^6 events were collected with a trigger of greater than nine particles in trigger detector TD . A portion of the data was acquired in the absence of the field and used in our study.

The drift chambers are blown by a gas mixture $\text{Ar}(70\%) + \text{CO}_2(30\%)$ at atmospheric pressure. A voltage of 1.65 kV is applied to the anode. In spills with an intensity of 10^6 s^{-1} , the total current in the tracker is $30 \mu\text{A}$.

The detector status is monitored in the course of data acquisition by means of control histograms filled by the data acquisition program in intervals between accelerator cycles. The monitored parameters of each chamber are (i) the number of tubes activated in a particular event, (ii) the TDC spectrum, (iii) the distribution of hits over the tubes, and (iv) the distribution of hits in clusters.

CALIBRATION OF THE DRIFT TUBES

A TDC reading provides a means for determining distance r between the anode wire and the track passing through the tube. This is done using the tabulated dependence of r_i , where subscript i denotes readings of the TDC samples and defines drift time t . Dependence r_i is determined for each DT tube from the TDC distribution without recourse to the data from the other tracking detectors.

If the distribution of events over r is uniform, equation $r/r_0 = P(t)$ holds true for the time dependence of drift radius $r(t)$ (r_0 is the maximum drift length, i.e., the inner radius of the tube; t is the TDC sample; and $P(t)$ is the distribution function of time, i.e., the probability of detecting it in the interval from 0 to t). Hence, it follows that calibration function $r(t) = r_0 P(t)$ can be obtained from the known time distribution.

In this experiment, tracks are uniformly (with a high accuracy) distributed along r . Even when the particle beam changes essentially on the width of one tube (but is dependent on r according to a linear law), the uniformity is restored by summing the distributions of tracks passing on the left and on the right of the anode wire. Assuming that particles are uniformly distributed along radius r

$$\frac{dn}{dr} = \rho = \text{const}, \quad (1)$$

we can relate density ρ to the total number of particles detected in this tube:

$$N_{\text{tot}} = \int_0^{r_0} \frac{dn}{dr} dr = r_0 \rho. \quad (2)$$

From Eqs. (1) and (2), we obtain the expression for sought function $P(t)$, which involves the observed density of time distribution of events $\frac{dn}{dt}$:

$$P(t) = \frac{1}{N_{\text{tot}}} \int_{t_{\min}}^t \frac{dn}{dt} dt, \quad (3)$$

where t_{\min} is the minimum TDC sample.

Let us introduce the following notations: $i_1 \sim t_{\min}$ and $i_2 \sim t_{\max}$ are the minimum and maximum TDC samples, respectively. Denote the number of events with the i th TDC readout by $N_i \sim dn/dt$. For a system with a common “stop”, the number of samples in interval $i-i_2$ decreases as drift time i increases. Instead of $P(t)$ in Eq. (3), we use function P_i defined in the range of TDC readouts $i_1 < i < i_2$ by the formula

$$P_i = \sum_{j=i, i_2} (N_j - A) / \sum_{j=i_1, i_2} (N_j - A),$$

where A is the number of background events in one TDC sample.

Quantity $R_i = r_0 P_i$ makes sense of the drift radius for the i th TDC sample. The desired calibration is calculated according to the formula $r_i = 0.5(R_i + R_{i+1})$. To determine the operating TDC range, a region is selected in which P_i monotonously varies from 0.005 to 0.995; following that, one sample is added from the left and from the right. The example of the TDC distribution and the calibration dependence obtained on the basis of it for one tube is shown in Fig. 3.

Uniformity condition (1) for the event distribution in r is violated when a few tracks pass through the tube, but only one track proximate to the anode wire is recorded. Correction Δr for overlapped tracks is introduced into the calibration dependence according to the formula

$$\Delta r = \eta r(r/r_0 - 1),$$

where η is the fraction of two-track events.

In the data used for calibration, the value of parameter η is ≤ 0.2 .

The statistical error of calibration depends on number N of acquired events as $\sigma_R = r_0 / \sqrt{12N}$. From this, it follows that 1000 hits of the tube must be recorded to perform calibration with an accuracy of $30 \mu\text{m}$.

COORDINATE RESOLUTION

Two methods were used to measure the coordinate resolution of the drift tubes. One of these does not imply track reconstruction, and the other involves

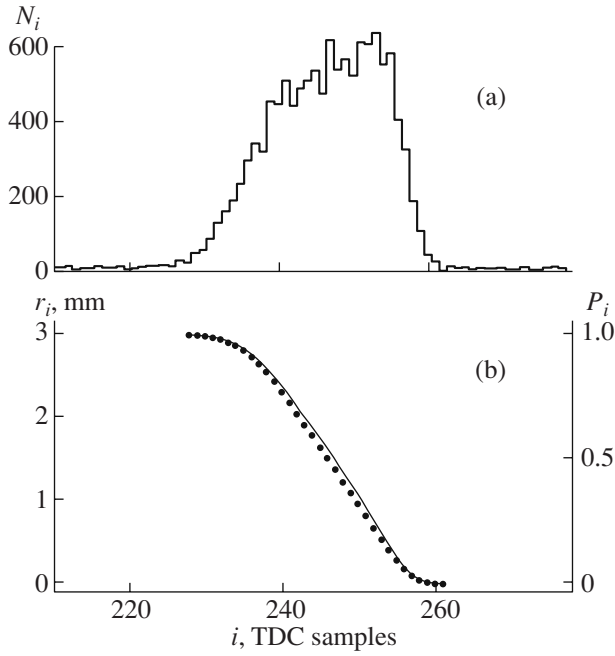


Fig. 3. (a) Distribution of TDC samples in the 70th tube of chamber U_1 and (b) calibration function for this tube before (a solid line) and after (dots) the correction for double coincidences was introduced.

reconstruction in the Y planes of the PVD and DT. The first method is illustrated in the inset in Fig. 4. In this case, drift lengths r_1 and r_2 in the overlapping tubes of two adjacent planes $Pl1$ and $Pl2$ are measured. Tracks of particles from a remote point target may pass through region A or B . In region A , segments r_1 and r_2 are located on the both sides of the measured track. One can easily see that $r_1 + r_2 \approx \text{const}$. In region B , segments r_1 and r_2 lie on the same side from the track and $r_1 - r_2 \approx \text{const}$.

To estimate the resolution, we selected only those pairs of tubes in which overlaps in the difference mode were absent. The characteristic distribution of $r_1 + r_2$ is shown in Fig. 4. To reduce the background level, we rejected events in which, apart from the tubes at hand, adjacent tubes were also hit. The distributions are described by the function

$$f(x) = a_n \exp\left(-\frac{(x - x_n)^2}{2\sigma_n^2}\right) + a_w \exp\left(-\frac{(x - x_w)^2}{2\sigma_w^2}\right),$$

where the first term represents the narrow peak due to tracks from the target and the second describes the wide background component. Parameter σ_n constitutes quadratic sums of two independent measurements; therefore, the resolution of one tube is evaluated according to the formula $\sigma_r = \sigma_n / \sqrt{2}$. For the majority of tubes, σ_r is in the range of 280–350 μm .

The resolution of the tubes in chambers Y_1 , Y_2 , and Y_3 was also estimated by the offsets of tracks. Tracks

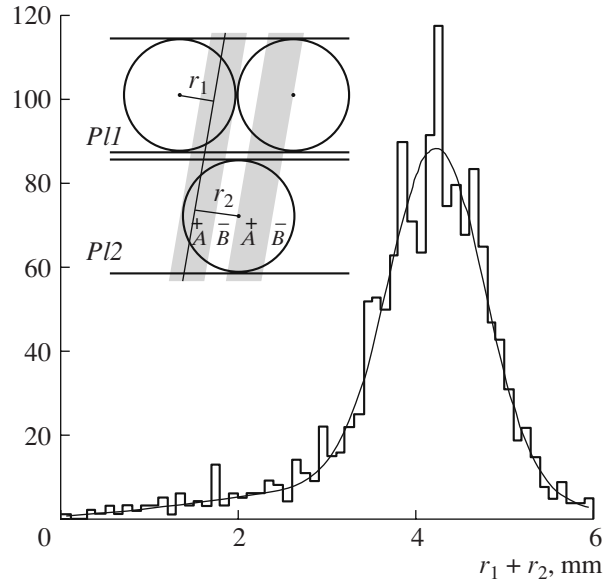


Fig. 4. Distribution $r_1 + r_2$ for a pair of tubes. The regions corresponding to the sum and difference modes are shown in the inset.

recognized in the PVD are extended into the DT by minimizing the function

$$\chi^2(\xi) = \left(\frac{\xi}{\sigma_\xi}\right)^2 + \sum_{i=1}^n \left(\frac{r_i - r'_i(\xi)}{\sigma_r}\right)^2$$

with respect to kink angle ξ (r' is the distance from the reconstructed track to the tube axis).

A kink occurs in the plane of the final strip detector and is introduced into the expression to take into account multiple scattering of particles. The averaged value $\sigma_\xi = 1$ mrad is used in the analysis of the coordinate resolution. Summation is performed over n planes of the DT with $\sigma_r = 0.3$ mm.

To determine offset δ in the specified DT plane, tracks are reconstructed in the other five planes. Selected are tracks originating from vertices located inside the hydrogen target with $\chi^2/5 < 1.5$. The offset is determined by the expression $\delta = \pm(r' - r)$, in which the sign “+” or “-” indicates the side from the anode wire on which the track is located. The distribution of the offset is described by the function

$$y = a_0 + a_1 \exp\left(-0.5 \left(\frac{\delta}{\sigma_\delta}\right)^2\right).$$

Intrinsic resolution of the tube σ_{tube} is determined from resolution of the offset σ_δ : $\sigma_{\text{tube}} = \sqrt{\sigma_\delta^2 - \sigma_{\text{track}}^2}$. Parameter σ_{track} was estimated for three Y chambers during simulation of the setup using the PYTHIA generator of pp interactions and the GEANT 3.21 software package, which propagates tracks through the experimental setup. The component of the resolution due to

Parameters of the particle detection efficiency

Parameter	Chamber		
	Y_1	Y_2	Y_3
$\varepsilon_{av}, \%$	99.64 ± 0.27	99.75 ± 0.28	99.32 ± 0.27
$\Delta, \mu\text{m}$	183 ± 3	156 ± 3	166 ± 3
$\varepsilon_0, \%$	94.0	94.9	94.6

the gas and the electronics is assumed to be 0.3 mm for all tubes. The average values of σ_{track} and σ_{tube} in the Y chambers are as follows:

	Y_1	Y_2	Y_3
$\langle \sigma_{\text{track}} \rangle, \text{mm}$	0.13	0.15	0.24
$\langle \sigma_{\text{tube}} \rangle, \text{mm}$	0.29	0.27	0.30

Tracks reconstructed when measuring the coordinate resolution are also used to analyze the detection efficiency of the tubes. Tracks passing at distance $r \leq 1.5$ mm from the center of a tube are selected. The response of this tube is tested in the TDC range with a width of 32 samples. Averaged values of the measured efficiency near the anodes ε_{av} are presented in the table.

To describe total efficiency ε of a plane, we check whether at least one of the two tubes adjacent to the track is triggered. At a high detection efficiency near the anodes, counting losses in the plane mostly occur in the region near the walls. Therefore, in the first approximation, the value of ε is determined by the effective thickness of the wall or width Δ of the insensitive region according to the formula

$$\varepsilon(\alpha) = 1 - \Delta / (\cos(\alpha)R_{\text{out}}),$$

in which α is the track inclination with respect to the beam and R_{out} is the outer radius of the tube.

The values of Δ obtained while describing dependence $\varepsilon(\alpha)$, as well as efficiencies ε_0 of the planes at a frontal incidence of the beam ($\alpha = 0$), are presented in the table.

CONCLUSIONS

A tracker based on 6-mm-diameter drift tubes has been developed and tested. The accuracy with which

the coordinate is measured by one tube from the drift time is 0.27–0.30 mm. The detection efficiency for relativistic particles at a distance of <1.5 mm from the anode wire is >99%. The counting loss of one layer of tubes is governed by the thicknesses of the walls and adjacent insensitive region; it makes up ~5% of the layer area. The particle detection efficiency of two layers of tubes (i.e., of the chamber as a unit) is close to 100%.

ACKNOWLEDGMENTS

We thank the team of the U-70 accelerator complex for the high-quality beam extraction, as well as T.P. Topuriya, a staff member at the Laboratory for Particle Physics of the Joint Institute for Nuclear Research, for his managerial support during development of the detector.

This work was supported by the Russian Foundation for Basic Research, grant nos. 06-02-81010-Bel_a and 06-02-16954.

REFERENCES

1. Basiladze, S.G., Vorob'ev, A.P., Ermolov, P.F., et al., *Preprint of Institute of Nuclear Physics, Moscow State University*, Moscow, 1999, no. 99-28/586.
2. Ermolov, P.F., Kuraev, E.A., Manjavidze, J., et al., *Phys. At. Nucl.*, 2004, vol. 67, no. 1, p. 108.
3. Ardashev, E.N., Babintsev, V.V., Bogdanova, G.A., et al., *Prib. Tekh. Eksp.*, 2001, no. 4, p. 31.
4. Ardashev, E.N., Bogdanova, G.A., Volkov, V.Yu., et al., *Preprint of Institute of Nuclear Physics, Moscow State University*, Moscow, 2005, no. 2005-14/780.
5. Bychkov, V.N., Faessler, M., Geyer, R., et al., *Part. Nucl. Lett.*, 2002, no. 111, p. 64.
6. Bychkov, V.N., Dedek, N., Dunnweber, W., et al., *Nucl. Instrum. Methods Phys. Res. A*, 2006, vol. 556, p. 66.
7. Viriasov, K.S., Gusakov, Ju.V., Zhukov, I.A., et al., *Preprint of Joint Institute for Nuclear Research*, Dubna, 2005, no. E13-2005-127.
8. Alexeev, G.D., Baturitsky, M.A., Dvornikov, O.V., et al., *Nucl. Instrum. Methods Phys. Res. A*, 2001, vol. 462, p. 494.
9. Sen'ko, V.A. and Yakimchuk, V.Ya., *Preprint of Institute for High Energy Physics*, Protvino, 1995, no. 95-105.